

# Failure analysis of the PPS-based bag filters in coal-fired power plants:a surface structural evolution insight

Bing Zhang<sup>1</sup>, Wei Wang<sup>2</sup>, Zhihong Zheng<sup>3</sup>, Jingyun Zhang<sup>4</sup>, Yuekun Lai<sup>2</sup>, Jianying Huang<sup>2</sup>, Hong Cao<sup>2</sup>, and Weilong Cai<sup>1</sup>

<sup>1</sup>Qingyuan Innovation Laboratory

<sup>2</sup>Fuzhou University

<sup>3</sup>Xiamen University

<sup>4</sup>Xiamen Savings Environmental Co., LTD.

February 22, 2024

## Abstract

Owing to the complicated environments, the service life of bag-filter or electrostatic-bag composite precipitators with polyphenylene sulfide (PPS)-based bag-filter materials is greatly deviated from the ideal time. In this paper, the structural transformation of PPS-based bag filter materials collected from the coal-fired power plants with different loading units were investigated systematically. As the SO<sub>2</sub> content increases, the surface evolution of PPS fibers from smoothness to crack occurs. The major reason for the failure of PPS-based bag filters is that working temperature (T) often passes through acid dew gas point (Ta), and the SO<sub>3</sub> would be produced during the condensing of H<sub>2</sub>SO<sub>4</sub> when T is lower than Ta. This work discloses the actual structural evolution of PPS and some corresponding rules under the complicated corrosive gases with high temperatures, which provides a guidance for prolonging the service life of PPS-based bag filters during the usage of coal-fired power plant

## 1. Introduction

Recently, release standards of the atmospheric particulate pollution became more and more strict [1-5]. As a main source of particulate pollution, flue gas containing NO<sub>x</sub>, SO<sub>x</sub> from coal-fired power plants needs to be handled carefully. As a feasible and cost-effective dust removal technology, bag-filter or electrostatic-bag composite precipitators with polyphenylene sulfide (PPS)-based bag-filter material have attracted numerous attentions from researchers and relative industrial engineers because of its high rejection rate, low resistance and easy cleanout [6-11]. A critical and limited parameter of precipitators is the lifetime, which is closely related to the operating cost of factories. Besides, the lifetime of PPS with high resistance to aggressive chemicals and high temperature is dominate in the durability of precipitators [12-16]. The designed life of a PPS-based filter bag could reach to 5 years under ideal conditions. In practice, the lifetime can range from 8 months to several years in coal-fired power plants owing to its complicated environments [1, 17].

Compared with PTFE, PET or other polymer materials [18-20], the C-S bond in the PPS chains is easily oxidized into sulfoxide and sulfone groups, and even broken under the high temperature and acid corrosion [21-23]. Consequently, the reduced mechanical properties, shorter service life can be observed. Extensive researches [24-27] have been conducted to illustrate the degradation mechanisms of PPS under the simulated environments. Tanthapanichakoon [8] examined the resistance of a PPS-based filter to several chemicals, concluding that HNO<sub>3</sub> caused severe degradation of the PPS filter while remaining highly resistant to HCl and H<sub>2</sub>SO<sub>4</sub>. Besides, they also discovered that the mechanical properties of PPS material become poor at the atmosphere [28]. Cai [29] investigated that oxidation degradation of PPS can be aggravated with the increase in H<sub>2</sub>SO<sub>4</sub> dew point. Moreover, the effect of mixtures of NO and O<sub>2</sub> [30], NO<sub>2</sub> and SO<sub>3</sub> [9] on

the degradation of PPS have also been put forward. Although the effects of several chemical species on the degradation of PPS have been interpreted to a certain degree, the influence or substantial effect of SO<sub>2</sub> and O<sub>2</sub> gases at high temperature has not been well understood. Moreover, it is worth mentioning that the previous works about the degradation of PPS are executed under the normal environments, but the intricate environment with flue gas from coal-fired power plants containing multiple corrosive gases such as NO, NO<sub>2</sub>, SO<sub>2</sub>, SO<sub>3</sub>, O<sub>2</sub> and so on has never been explored. The effects of corrosive gases and corresponding rules in actual engineering projects are lacking and need to be further explored.

In this work, scanning electron microscope (SEM), differential thermal analysis (DTA), fourier transform infrared spectroscopy (FT-IR) and electronic fabrics strength tester (CRE) are employed to analyze the structural transformation of PPS-based bag filter materials collected from the coal-fired power plants. The effects of SO<sub>2</sub> and O<sub>2</sub> gases at high temperature were also investigated. The work would explain the actual structural evolution of PPS and mechanisms under the complicated corrosive gases with high temperatures, which will provide a guidance for prolonging the service life of PPS-based bag filters during the usage of coal-fired power plants.

## 2. Experimental

### 2.1 Materials and related details

Fifteen PPS-based bag filter materials were kindly provided by Xiamen Savings Environmental Co., Ltd., which were collected from coal-fired power plants with various loading units in China. According to the power of loading units, above samples could be classified into three categories: below 200 MW (sample 1#-5#), 200-300 MW (sample 6#-10#) and above 300 MW (sample 11#-15#).

Table 1. Sample labels and related parameters under the loading units below 200 MW.

samples	1#	2#	3#	4#	5#
Loading units / MW	150	100	100	10	60
SCR system	working	working	working	working	working
Dust collector type	electro-bag	pure bag	pure bag	electro-bag	electro-bag
Materials	PPS/PPS	PPS/PPS	PPS/PPS	PPS/PPS	PPS/PPS
Temperature of flue gas /	115.8-117.7	162.5-164.9	128.4-130.6	130.7-136.5	165.3-170.9
Content of O <sub>2</sub> / %	7.20-7.55	5.69-6.76	6.13-6.73	7.22-9.66	3.73-4.52
Content of SO <sub>2</sub> / mg·m <sup>-3</sup>	661-1330	1418-1604	1464-1670	1537-2265	5800-8806
Service time / month	66	24	31	20	6
Status of bag filter	using	using	partial failure	partial failure	complete failure

Note: using, partial failure and complete failure of the status of bag filter were defined as failure rate of that below 3%, 3-30% and above 30%, respectively.

The flue gas containing NO<sub>x</sub>, SO<sub>x</sub>, dust particles from combustion tower was emitted to the atmosphere after processing with denitration, dedusting and desulphurization in sequence, and the detailed information was shown in Fig. 1. Samples collecting from factories were placed in the step of dedusting under the temperature of 110-180 after NO<sub>x</sub> was removed from flue gas through denitration. The bag filter would execute the operation of cleaning when the resistance of that reach to the critical point, and thus could be used repeatedly unless the filter was damaged completely. The corresponding information of samples with different loading units was summarized and shown in Table 1 (below 200 MW), Table 2 (200-300 MW) and Table 3 (above 300 MW), respectively.

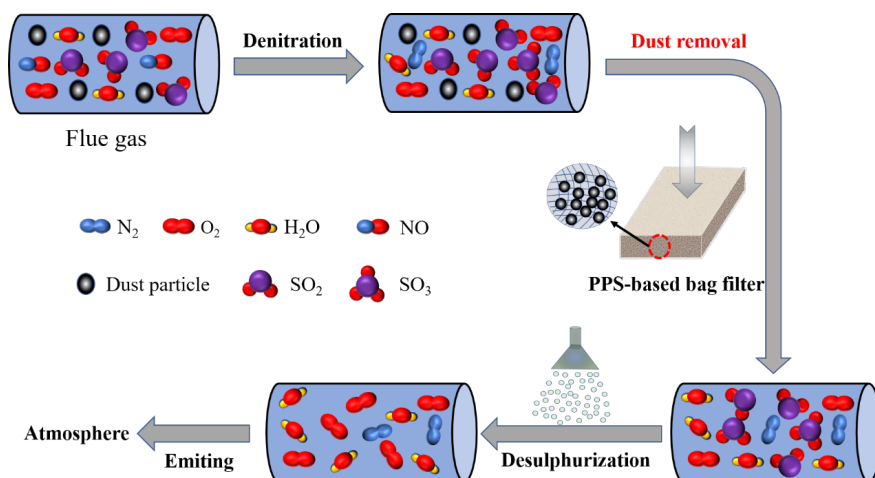


Figure 1. The treatment processes of flue gas in coal-fired power plants.

## 2.2 Characterizations

The surface morphology of PPS-based bag filter materials was observed by a scanning electron microscope (SEM, HBS-100A, Shanghai Tianjing Co., China). Samples were cut randomly from the bulk of bag filter, and then coated with gold sputters before testing.

Table 2. Sample labels and related parameters under the loading units between 200MW and 300 MW.

samples	6#	7#	8#	9#	10#
Loading units / MW	300	300	300	210	300
SCR system	working	working	working	working	working
Dust collector type	pure bag	electro-bag	pure bag	electro-bag	electro-bag
Materials	PPS/PTFE	PPS/ PTFE	PPS/PPS	PPS/ PTFE	PPS/ PTFE
Temperature of flue gas /	117.1-123.7	126.0-128.5	117.9-127.0	139.4-141.6	170-173.5
Content of O <sub>2</sub> / %	4.68-5.90	5.59-6.42	6.05-6.45	5.48-7.23	4.37-5.57
Content of SO <sub>2</sub> / mg·m <sup>-3</sup>	616-1076	1630-1716	1974-2571	3090-5042	6146-6753
Service time / month	21	20	24	29	15
Status of bag filter	using	using	partial failure	partial failure	partial failure

Note: using, partial failure and complete failure of the status of bag filter were defined as failure rate of that below 3%, 3-30% and above 30%, respectively.

The functional structure evolutions of PPS-based bag filter materials under the practical environments were detected by a FTIR spectrometer (WQF-510, Beijing Rayleigh Analytical Instrument Co., China) equipping with a single reflection attenuated total reflectance (ATR, PIKE, America) accessory. The spectral resolution of 4 cm<sup>-1</sup>, the range of 4000-400 cm<sup>-1</sup> and scan times of 32 were adopted at ambient temperature. At the same time, the melting points of above samples were monitored by a thermal analyzer system (ZCT-B, Beijing JYGK Instrument Co., China). The samples were heated from 100 to 400 with a constant ramping rate of 10 /min at air atmosphere. Besides, the samples were sealed previously into aluminum pans with approximately 10 mg before measuring.

Table 3. Sample labels and related parameters under the loading units above 300 MW.

samples	11#	12#	13#	14#	15#
Loading units / MW	350	350	330	600	330
SCR system	working	working	working	working	working
Dust collector type	pure bag	electro-bag	pure bag	electro-bag	pure bag
Materials	PPS/PPS	PPS/PPS	PPS/PPS	PPS/PPS	PPS/PPS
Temperature of flue gas /	122.0-125.0	117.1-120.3	124.3-126.6	115.9-117.5	129.3-132.7
Content of O <sub>2</sub> / %	5.72-7.29	3.84-6.46	4.00-6.53	4.89-5.38	7.10-9.16
Content of SO <sub>2</sub> / mg·m <sup>-3</sup>	1161-1441	1516-1670	1530-2100	2030-2600	3312-4081
Service time / month	22	32	30	26	6
Status of bag filter	using	using	partial failure	partial failure	partial failure

Note: using, partial failure and complete failure of the status of bag filter were defined as failure rate of that below 3%, 3-30% and above 30%, respectively.

The cross breaking (CD) strength of samples was tested by an electronic fabrics strength tester (YG026C, Changzhou textile instrument Co., China). The gauge length and extension rate were set as 200mm and 100mm/min according to the testing method for nonwovens-Part 3: Determination of tensile strength and elongation, MOD (ISO 9073-3), respectively. The 300×50 mm strips cut from PPS-based bag filter materials were adopted to operate for related measurement. Every sample was tested for 5 times and average values were used to illustrate the changes of transverse strength of bag filters.

### 3. Results and discussion

#### 3.1 Morphologies of PPS-based bag filter materials

SEM images of PPS-based bag filter materials collecting from coal-fired power plants with different loading units were shown in Fig. 1. A three-dimensional interpenetrated configuration is easily observed for all samples regardless of loading units of coal-fired power plants, which is built by stacking of PPS fibers through nonwoven technology to furnish the bag filter with open-cells pores and high porosity. The existence of above network makes it possible to filter dust particles effectively for PPS-based bag filters with excellent dust rejection rate.

When the loading units is below 200 MW (sample 1#-5#), the relatively smooth surface along the fiber axis accompanying with little particles is observed for sample 1# and 2#. While the regular cracks liking knife cuts that vertical to the fiber axis appear for sample 3#, 4# and 5#. From Table 1, the status of bag filters changes from using to complete failure for sample 1#-5#, indicating that the evolution of surface of PPS-based bag filter materials from smooth to cracked occurs as failure degree increases, which is in line with the content variation of SO<sub>2</sub> in the system and would be discussed in detailed in section 3.4. The depth of cracks becomes more intensified for completely

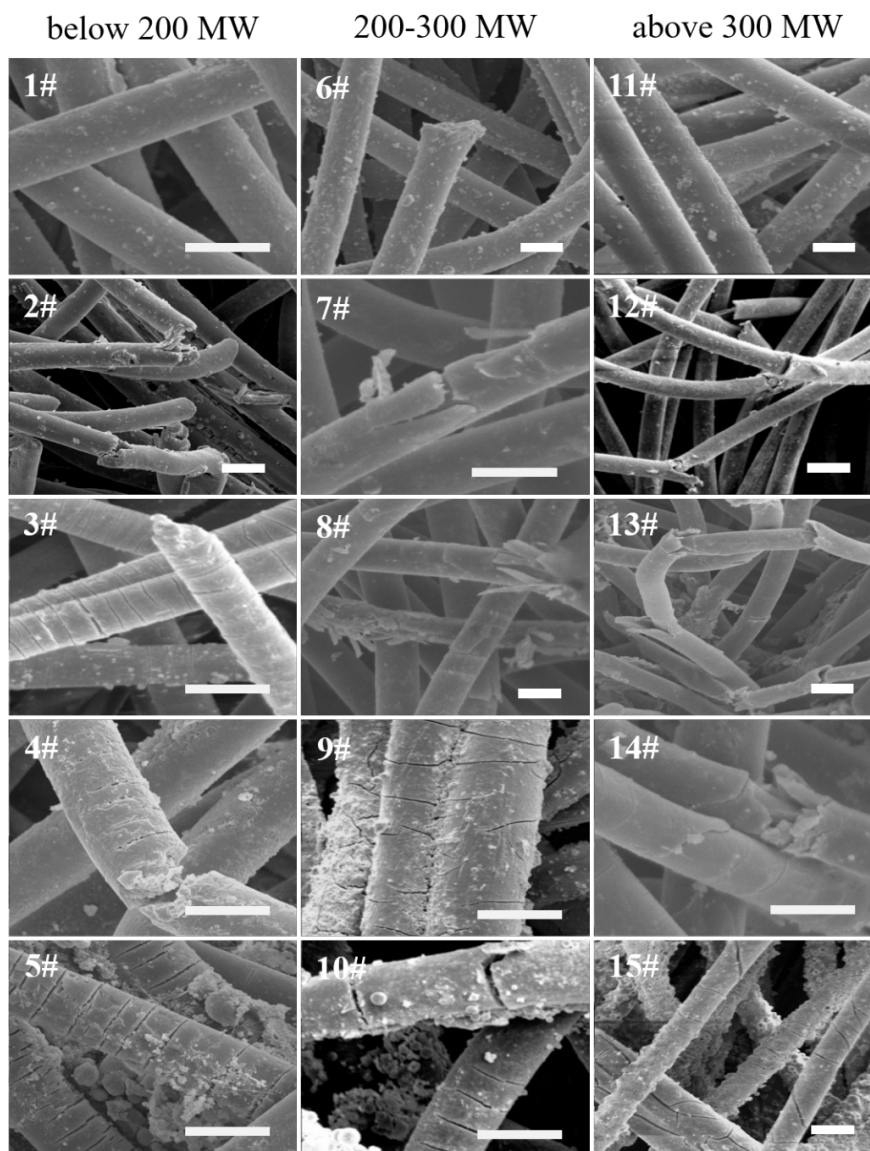


Figure 2. SEM images of PPS-based bag filter materials with different loading units (All the bars are 10 $\mu$ m). failure sample (5#) than partly failure sample (3# and 4#), showing that the cracks would extend with the increase of the content of SO<sub>2</sub>. In other words, the higher content of SO<sub>2</sub> is, the larger depth of cracks is, the deeper damage of the fiber is. Besides, the service life of 5# is deeply destroyed below 200 MW is only 6 months, while that of 1# and 2# is more than 20 months, indicating that the structure transformation of fiber surface has nothing to do with the service life in factories.

The same trend of structural evolution on fiber surface was observed with the addition of SO<sub>2</sub> content for samples loading units between 200 and 300 MW (sample 6#-10#) and above 300 MW (sample 11#-15#). This illustrates that the loading unit of coal-fired power plants is independent of the variation of fiber surface. It's worth mentioning that the dust particles are attached to the fiber surface for all samples. Commonly, the dust particles would be removed from the network of bag filter by the cleaning operation, and the fiber surface should be smooth in accordance with the original morphology of PPS fibers. The appearance of particles on the fiber surface indicates that the roughness of fibers becomes obvious with the occurring of

fiber degradation[9, 31], the interaction between the fiber and particles increases with absorbance of particles on the fiber surface, and thus above phenomenon can be explained. The absorbance of particles around the fiber is larger for sample 5#, 9#, 10# and 15#, whose SO<sub>2</sub> content are higher as 4000 mg/m<sup>3</sup> than other samples, and this is consistent with the degradation degree of PPS-fiber in the working conditions. The higher the content of SO<sub>2</sub> is, the larger degradation degree is, the rougher of fiber surface is, and thus the easier of particle adsorption becomes. Besides, the trapped particles would increase the filtration resistance in the following cycling process of dust removal, thus the performance of bag filters becomes worse with the increase of SO<sub>2</sub> content in the system.

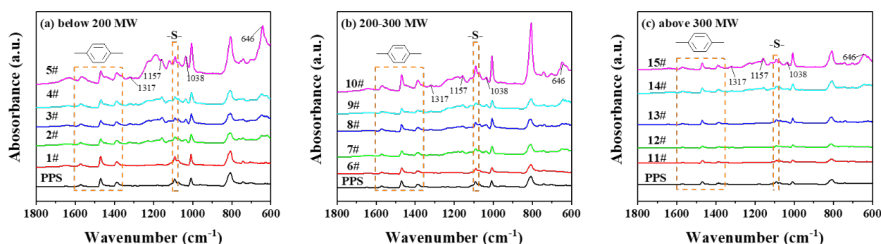


Figure 3. FT-IR patterns of PPS-based bag filter materials with different loading units.

### 3.2 Chemical evolutions of PPS-based bag filter materials

In order to obtain the configuration change of PPS bag filter materials with various loading units in coal-fired power plants, ATR-FTIR was conducted directly and related data were shown in Fig. 3. Besides, main changes in the characteristic peaks of PPS-based bag filter materials with loading units below 200 MW, 200-300 MW and above 300MW were summarized from Fig. 3 and displayed in Table 4, Table S1 and Table S2, respectively.

The characteristic peaks of in-plane stretching vibration of C-C bond in the benzene ring at 1572 cm<sup>-1</sup>, 1470 cm<sup>-1</sup> and 1386 cm<sup>-1</sup> and the stretching vibration of C-S bond at 1092 cm<sup>-1</sup> are observed for all samples, which are originated from the bulk materials of PPS[7, 32, 33]. The new peaks of the stretching vibration of -SO- at 1036 cm<sup>-1</sup> and the stretching vibration of -SO<sub>2</sub>- at 1157 cm<sup>-1</sup>, and 1321 cm<sup>-1</sup> appear for sample 2#-5# compared with pure PPS (Table 4), indicating that the oxidation of C-S bond into sulfoxide (-SO-) and sulfone (-SO<sub>2</sub>-) in PPS molecule happens at high temperature when the content of SO<sub>2</sub> is more than 1500 mg/m<sup>3</sup>. However, only an extremely weak peak at 1163 cm<sup>-1</sup> belonging to -SO<sub>2</sub>- is detected for sample 1#, showing that the degree of oxidation of sample 1# is lower than that of sample 2#-5#. Besides, the new peak of the stretching vibration of -SO<sub>3</sub>H at 646 cm<sup>-1</sup> emerges and becomes stronger with the addition of content of SO<sub>2</sub>(from 1# to 5#). The appearance of new peak at 646 cm<sup>-1</sup> indicates that the hydrogen in the benzene ring could be replaced by sulfonic acid group through sulfonation[29]. At the same time, the sulfonation becomes obvious with the content of SO<sub>2</sub> adds and above phenomenon can be illustrated. Also, the new peaks representing the oxidation (1036 cm<sup>-1</sup>, 1157 cm<sup>-1</sup>, and 1321 cm<sup>-1</sup>) appear earlier than that on behalf of sulfonation (646 cm<sup>-1</sup>) with the increase of content of SO<sub>2</sub>, showing that oxidation is easier to take place than sulfonation in actual operating environment. The bond strength of C-S bond is the lowest in the PPS molecule[34], making it easier to be oxidized into sulfoxide (-SO-) and sulfone (-SO<sub>2</sub>-) at high temperature than converting hydrogen into sulfonic acid group in the benzene ring.

Table 4. Main changes in the characteristic peaks of PPS-based bag filter materials with the loading units below 200 MW.

samples	C-S in-plane stretching vibration	-SO-stretching vibration	-SO <sub>2</sub> - stretching vibration	-SO <sub>2</sub> - stretching vibration	-SO <sub>3</sub> H Stretching vibration
PPS	1092	-	-	-	-

samples	C-S in-plane stretching vibration	-SO-stretching vibration	-SO <sub>2</sub> - stretching vibration	-SO <sub>2</sub> - stretching vibration	-SO <sub>3</sub> H Stretching vibration
1#	1092	-	1163 (Weaker)	-	-
2#	1090	1038 (Weak)	1157 (Strong)	1321 (Weak)	646 (Strong)
3#	1090	1036 (Strong)	1157 (Strong)	1321 (Weak)	646 (Strong)
4#	1090	1036 (Strong)	1157 (Strong)	1319 (Weak)	646 (Strong)
5#	1090	1036 (Stronger)	1159 (Strong)	1319 (Weak)	642 (Stronger)

When the loading units of coal-fired power plants change from below 200 MW to 200-300 MW and above 300 MW, the similar variations of new peaks are obtained with the increase of content of SO<sub>2</sub>. These results further verified the variation of PPS molecule under the corrosive atmospheres is irrelevant to loading unit, which is coincide with the conclusions acquired from SEM images.

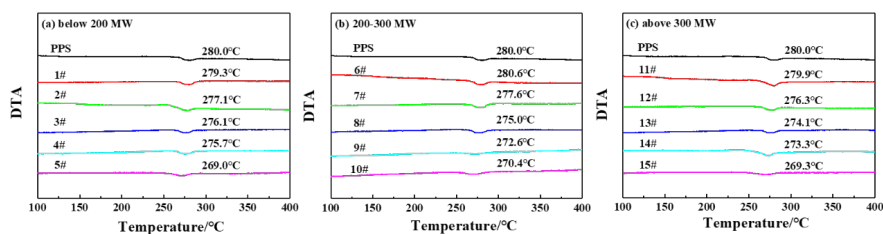


Figure 4. DTA patterns of PPS-based bag filter materials with different loading units.

As a key indicator for the semi-crystalline of PPS, the melting point ( $T_m$ ) could reflect intuitively its crystalline characteristics[27]. DTA patterns of pure PPS and fifteen samples collecting from factories were conducted by a thermal analyzer system and summarized in Fig. 4. It can be observed that  $T_m$  reduces progressively and the width of peak of melting point becomes broaden with increase of content of SO<sub>2</sub> for all categories regardless of loading unit (below 200 MW, 200-300MW and above 300 MW). Generally, crystal is an ordered arrangement of molecular chains, while the melting destroys the assembly structure of molecules wholly to form the disordered molecular chain[27, 35]. Higher crystallinity of polymer is, more regular of arrangement of molecular chains is, and higher temperature to destroy its assembly structure needs, and thus higher the melting point gets for the same material. The appearance of new functional groups including -SO-, -SO<sub>2</sub>- and -SO<sub>3</sub>H in the molecular chain of PPS would break its structural regularity along with the decreasing of crystallinity, and reduction of melting point of fifteen samples can be explained. Besides, the lower of melting point is, the more serious damage of crystal is, and thus the lower of crystallinity is for the same material. Therefore, the crystallinity of PPS gradually declines with the addition of content of SO<sub>2</sub> from 1# to 5#, 6# to 10# and 11#-15#, which is in good agreement with those obtained from the SEM and FTIR analysis.

### 3.3 Mechanical properties of PPS-based bag filter materials

As a crucial index to evaluate superiority or inferiority of mechanical properties of PPS-based bag filter materials during the running of the filter bag, CD strengths of all samples were introduced and shown in Fig. 5.

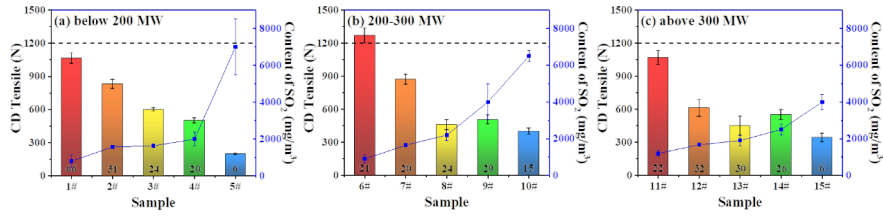


Figure 5. The variations of CD strength of PPS-based bag filter materials with different loading units.

According to the GB/T 6719, the CD strength of filter bags should more than or equal to 1200 N, while the CD strengths of all samples except 6# are lower than that value indicating that all samples are subject to degradation under the complicated and corrosive atmospheres. CD strength decreases for three categories (below 200 MW, 200-300MW and above 300 MW) as the content of SO<sub>2</sub> increases independence of loading unit. Commonly, the tensile strength of bag filter is closely related to the crystallinity and defeats of PPS fiber adopted[35]. The tensile strength becomes larger with the increase of crystalline of PPS fiber, while declines with the addition of defeats which would turn into stress concentration points to accelerate the fracture of fiber. From the above analysis, the crystalline reduces and surface defeats of PPS fibers rises with the content of SO<sub>2</sub> increases, bringing down the CD strength of bag filter at the same time. Besides, it's worthwhile to notice that the CD strength of samples is lower than 600 N that nearly 50% loss of theoretically initial strength when the content of SO<sub>2</sub> is more than 1500 mg/m<sup>3</sup>, which can't afford the normal run of dedusting and cleaning resulting in the failure of bag filter.

### 3.4 Mechanisms of structure evolutions of PPS-based bag filter materials

The evolutions of structure and mechanical property of PPS-based bag filter materials with different loading units were clarified in detail, but the dominating factor bringing about above variations is unclear and needs to be further explained.

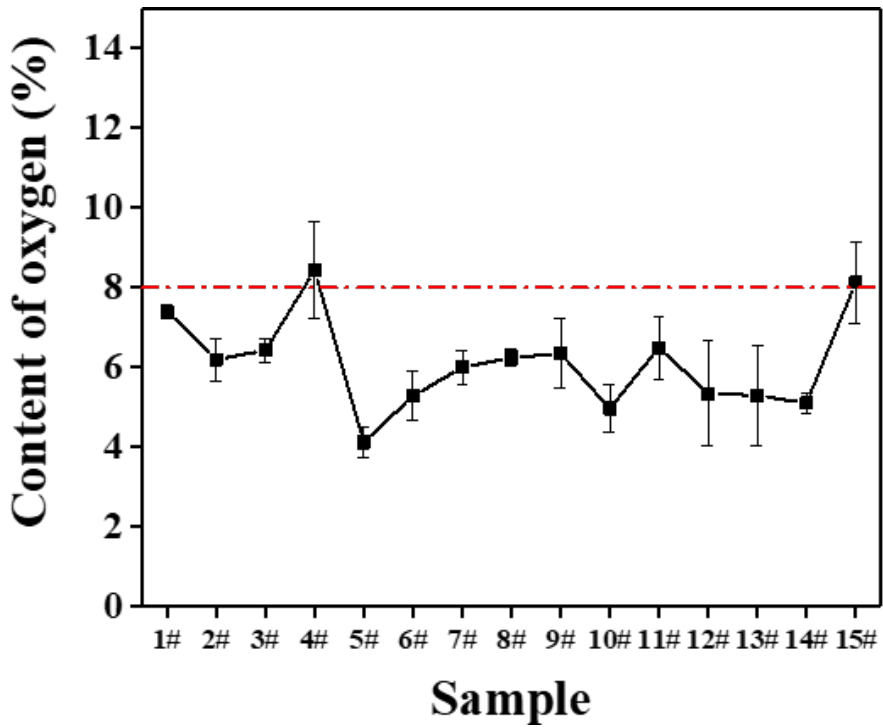
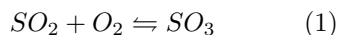


Figure 6. The variations of O<sub>2</sub> content of PPS-based bag filter materials with different loading units.

The variations of material structure and properties is bound up with the working conditions. The major duty parameters including temperature of flue gas, the content of O<sub>2</sub>, the content of NO<sub>x</sub>, the content of SO<sub>x</sub> and so on could cause damage to the PPS fibers in the coal-fired power plants. The effect of NO<sub>x</sub> can be ignored because all samples were collected from the system containing denitrification system with regular service. The O<sub>2</sub> content should be lower than 8% for the safety operation of PPS-based bag filter in the flue gas of coal-fired power plants based on the previous report [36]. The O<sub>2</sub> content for all samples is lower than 8% from Fig.6, making it negligible to influence the structure of PPS fibers. Therefore, the failure of PPS-based bag filter must exist closely relationships with the content of SO<sub>x</sub> and temperature of flus gas.



The major component in the SO<sub>x</sub> of flue gas is SO<sub>2</sub>, which could be oxidized into SO<sub>3</sub> under the assistance of O<sub>2</sub> at high temperature (eq (1)). The conversion rate from SO<sub>2</sub> into SO<sub>3</sub> is between 0.1% and 3% based on literature. SO<sub>3</sub> would combine with water in the flue gas to form vapor of H<sub>2</sub>SO<sub>4</sub> (eq (2)), and the acid gas dew point (condensing temperature) would increase with the addition of concentration of H<sub>2</sub>SO<sub>4</sub> vapor. When the temperature of flue gas reduces to the acid gas dew point, H<sub>2</sub>SO<sub>4</sub> vapor would condense into liquid concentrated H<sub>2</sub>SO<sub>4</sub>. Then, liquid concentrated H<sub>2</sub>SO<sub>4</sub> combines with flying ash in the flue gas and co-adheres to the three-dimensional network of bag filters. After that, dehydration reaction (eq (3)) occurs between molecules of H<sub>2</sub>SO<sub>4</sub> at high concentration to produce SO<sub>3</sub> with powerful oxidizing properties in the above network, resulting in the oxidation or even sulfonation of PPS-based bag filter. Therefore, the key point leading to the failure of PPS-based bag filters is the relationship between the temperature of flue gas and acid gas dew point.

$$T_a = 116.5515 + 16.06329 * \lg V_{SO_3} + 1.05377 * (\lg V_{SO_3})^2 \quad (4)$$

Where, V<sub>SO<sub>3</sub></sub> is the volume fraction of SO<sub>3</sub> in the flue gas (ppm).

Based on above conclusion, the eq (4) [37] was introduced to obtain the temperatures of acid gas dew point (T<sub>a</sub>) of coal-fired power plants which was fitted from Müller curve [38]. Considering the fluctuation of flue gas parameters and the diversity of influential factors of T<sub>a</sub>, T<sub>a</sub>s of fifteen coal-fired power plants were calculated on the basis of eq (4) with 0.1%, 1.5% and 3.0% of SO<sub>2</sub> conversion rates and marked as T<sub>0.1</sub>, T<sub>1.5</sub> and T<sub>3.0</sub>, respectively. The relationship between temperature of flue gas and T<sub>a</sub> was displayed in Fig. 7. It's easy to observe that running temperatures (T) of 1#, 6# and 11# are higher than relative T<sub>a</sub>, while running temperatures of 12 other coal-fired power plants are between T<sub>0.1</sub> and T<sub>1.5</sub>, hinting that T is often passing through T<sub>a</sub>. When T is higher than T<sub>a</sub>, H<sub>2</sub>SO<sub>4</sub> vapor produced from SO<sub>x</sub> couldn't condense on the surface of PPS fibers, and the oxidation of PPS fibers largely reduces which is beneficial to prolong the service life of bag filters in coal-fired power plants. Conversely, PPS fibers could be oxidized gradually with the increase of adhesion amount of liquid concentrated H<sub>2</sub>SO<sub>4</sub> when T is lower than T<sub>a</sub>. T<sub>a</sub> increases with the addition of SO<sub>2</sub> content in the flue gas, and the oxidation degree of PPS-based bag filters becomes deeper at the same time. Thus, above phenomenon can be illustrated. Besides, the SO<sub>2</sub> content in the flue gas is lower than 1500 mg/m<sup>3</sup> for 1#, 6# and 11#, which is a critical concentration of SO<sub>2</sub> that needs to be concerned especially for safety and long-time running of PPS-based bag filters in coal-fired power plants.

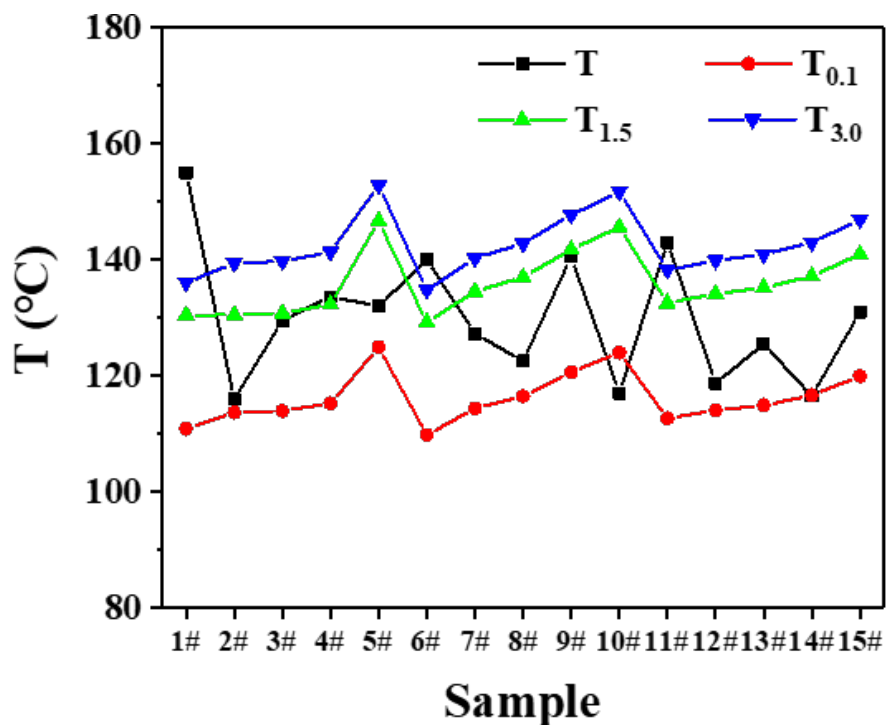


Figure 7. Relationships between temperature of flue gas and acid dew point of PPS-based bag filter materials with different loading units.

According to the above discussion, the possible failure mechanism of PPS-based bag filters in coal-fired power plants was proposed and shown in Fig. 8.

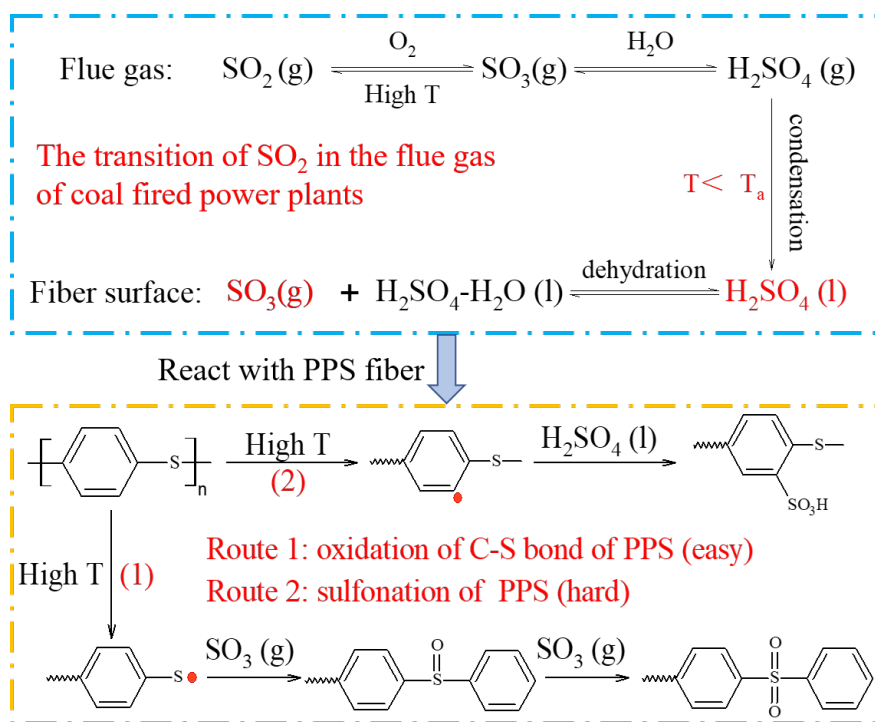


Figure 8. The failure mechanism of PPS-based bag filters in coal-fired power plants.

The  $\text{SO}_2$  in the flue gas would turn into  $\text{H}_2\text{SO}_4$  vapor under high temperature assisting with oxygen and water. Generally, the  $T_a$  is higher than  $T$ , but the  $T_a$  increases with the addition of  $\text{SO}_2$  content in the flue gas (Fig. 7). When the  $T$  is lower than  $T_a$ , the vapor converts into liquid for  $\text{H}_2\text{SO}_4$ , which combines with fly ashes and transports to the fiber surface in the three-dimensional network of PPS-based bag filter. Then, the strong oxidant of  $\text{SO}_3$  produced in the fiber surface through dehydration reaction. The  $\text{SO}_3$  would absorb on the surface of fiber and attack the C-S bond in the PPS chains inducing by high temperature (route (1)), which transforms into sulfoxide (-SO-) and sulfone (-SO<sub>2</sub>-). As the consumption of C-S bond reaches to a critical point, the hydrogen in the benzene ring of PPS could initiate and substitute by sulfonic acid group (-SO<sub>3</sub>H, route (2)). Moreover, the above reactions get intensified as the  $\text{SO}_2$  content increases. Therefore, the higher  $\text{SO}_2$  content is, the deeper oxidation is, the worse damage of fiber is, and thus the shorter lifetime of PPS-based bag filter in coal-fired power plants is.

#### 4. Conclusions

The structural transformation and variation of mechanical properties of PPS-based bag filter materials collected from the coal-fired power plants with different loading units were investigated by SEM, FTIR and TG. As the  $\text{SO}_2$  content increases in the flue gas, the oxidation degree of PPS fibers becomes deeper accompanying with transformation from oxidation of C-S bond to sulfonation of hydrogen in the benzene ring, and the surface evolution of above fibers from smooth to cracked occurs at the same time. But the melting point decreases with the addition of  $\text{SO}_2$  content, which is in accordance with the changing of crystalline of PPS-based bag filter materials. Thus, the reduction of crystalline and increasing of surface defects of PPS fibers brings down the CD strength of bag filter. The major reason causing the failure of PPS-based bag filter is as follows: working temperature ( $T$ ) is often passing through acid dew gas point ( $T_a$ ), the  $\text{SO}_3$  would be produced from condensing of  $\text{H}_2\text{SO}_4$  when  $T$  is lower than  $T_a$ . The  $\text{SO}_3$  with strong oxidation would attack the weak bonds of PPS, resulting in the oxidation or even sulfonation of PPS-based bag filters. Besides, the critical concentration of  $\text{SO}_2$  in the flue gas is lower than  $1500 \text{ mg/m}^3$ , which is beneficial for the safety and long-time running of PPS-based bag filters in coal-fired power plants.

**Supporting Information.** Corresponding data summarized from FTIR patterns are included in supporting information.

#### Acknowledgments

This work was financial supported by National Science and Technology Support Program (Grant No. 2015BAE01B04), the Talent Scientific Research Project of Qingyuan Innovation Laboratory (Grant No. 00521001) and the Platform Construction Project of Qingyuan Innovation Laboratory (Grant No. 00621005).

#### References

1. Ye, Y. and Z. Wang, *Effect of Corona Discharge on Polyphenylene Sulfide Filter Material of Electrostatic-Bag Composite Precipitators*. Industrial & Engineering Chemistry Research, 2018. **57** (4): p. 1319-1330.
2. Pui, D.Y.H., S.C. Chen, and Z.L. Zuo, *PM<sub>2.5</sub> in China: Measurements, sources, visibility and health effects, and mitigation*. Particuology, 2014. **13** : p. 1-26.
3. Jaworek, A., A. Krupa, and T. Czech, *Modern electrostatic devices and methods for exhaust gas cleaning: A brief review*. Journal of Electrostatics, 2007. **65** (3): p. 133-155.
4. Saleem, M., et al., *Experimental study of cake formation on heat treated and membrane coated needle felts in a pilot scale pulse jet bag filter using optical in-situ cake height measurement*. Powder Technology, 2011. **214** (3): p. 388-399.
5. Qian, Y., et al., *Effect of filtration operation and surface treatment on pulse-jet cleaning performance of filter bags*. Powder Technology, 2015. **277** : p. 82-88.

6. Huang, W., et al., *Effect of smoke components on polyphenylene sulfide filter medium of electrostatic fabric filter*. Polymer Materials Science & Engineering, 2013. **29** (11): p. 36-41.
7. Yan, P., et al., *Investigation on thermal degradation mechanism of poly(phenylene sulfide)*. Polymer Degradation and Stability, 2022.**197** : p. 109863.
8. Tanthapanichakoon, W., et al., *Mechanical degradation of filter polymer materials: Polyphenylene sulfide*. Polymer Degradation and Stability, 2006. **91** (11): p. 2614-2621.
9. Rozy, M.I.F., et al., *A continuous-flow exposure method to determine degradation of polyphenylene sulfide non-woven bag-filter media by NO<sub>2</sub> gas at high temperature*. Advanced Powder Technology, 2019.**30** (12): p. 2881-2889.
10. Li, H., Y. Diao, and Y. Zhang, *Thermal Dynamic Characteristics and Failure of PPS Filtering Fibers*. Journal of Donghua University. Natural Science Edition, 2012. **38** (2): p. 134-138.
11. Mao, N., et al., *Comparison of filter cleaning performance between VDI and JIS testing rigs for cleanable fabric filter*. Powder Technology, 2008. **180** (1): p. 109-114.
12. Yu, Y., et al., *Fabrication and application of poly (phenylene sulfide) ultrafine fiber*. Reactive and Functional Polymers, 2020.**150** : p. 104539.
13. Chen, G., A.K. Mohanty, and M. Misra, *Progress in research and applications of Polyphenylene Sulfide blends and composites with carbons*. Composites Part B-Engineering, 2021. **209** : p. 108553.
14. Yu, Y., et al., *Polyphenylene Sulfide Ultrafine Fibrous Membrane Modified by Nanoscale ZIF-8 for Highly Effective Adsorption, Interception, and Recycling of Iodine Vapor*. ACS Applied Materials & Interfaces, 2019. **11** (34): p. 31291-31301.
15. Gao, Y., et al., *Superhydrophilic poly(p-phenylene sulfide) membrane preparation with acid/alkali solution resistance and its usage in oil/water separation*. Separation and Purification Technology, 2018.**192** : p. 262-270.
16. Zhang, M., et al., *Preparation and properties of polyphenylene sulfide/oxidized-polyphenylene sulfide composite membranes*. Reactive and Functional Polymers, 2021. **160** : p. 104842.
17. Mukhopadhyay, A., V. Pandit, and K. Dhawan, *Effect of high temperature on the performance of filter fabric*. Journal of Industrial Textiles, 2015. **45** (6): p. 1587-1602.
18. Heo, K.J., et al., *High-performance bag filter with a super-hydrophobic microporous polytetrafluoroethylene layer fabricated by air-assisted electrospraying*. Science of The Total Environment, 2021. **783** : p. 147043.
19. Dong, W., et al., *Low-temperature silane coupling agent modified biomimetic micro/nanoscale roughness hierarchical structure superhydrophobic polyethylene terephthalate filter media*. Polymers for Advanced Technologies, 2022. **33** (5): p. 1655-1664.
20. Ma, Y., et al., *High heat resistance and good melt spinnability of a polyamide 66 containing benzene structure*. Materials Advances, 2021. **2** (20): p. 6647-6654.
21. Xing, J., Z.Z. Xu, and D.W. Li, *Preparation and oxidation resistance of polyphenylene sulfide modified by high-temperature antioxidants*. Materials Research Express, 2021. **8** (4): p. 045304.
22. Lian, D.D., et al., *Enhancing the resistance against oxidation of polyphenylene sulphide fiber via incorporation of nano TiO<sub>2</sub>-SiO<sub>2</sub> and its mechanistic analysis*. Polymer Degradation and Stability, 2016.**129** : p. 77-86.
23. Xing, J., et al., *Morphology and properties of polyphenylene sulfide (PPS)/polyvinylidene fluoride (PVDF) polymer alloys by melt blending*. Composites Science and Technology, 2016. **134** : p. 184-190.

24. Okubo, K., T. Sugeno, and H. Tagaya, *Chemical recycling of poly(p-phenylene sulfide) in high temperature fluids*. Polymer Degradation and Stability, 2015. **111** : p. 109-113.
25. Budgell, D.R., M. Day, and J.D. Cooney, *Thermal degradation of poly(phenylene sulfide) as monitored by pyrolysis-GC/MS*. Polymer Degradation and Stability, 1994. **43** (1): p. 109-115.
26. Yan, P., et al., *New insights into the memory effect on the crystallization behavior of poly(phenylene sulfide)*. Polymer, 2020.**195** : p. 122439.
27. Bulakh, N., J.P. Jog, and V.M. Nadkarni, *Structure development in curing of poly(phenylene sulfide)*. Journal of Macromolecular Science, Part B, 1993. **32** (3): p. 275-293.
28. Tanthapanichakoon, W., et al., *Degradation of bag-filter non-woven fabrics by nitric oxide at high temperatures*. Advanced Powder Technology, 2007. **18** (3): p. 349-354.
29. Cai, W.L. and G. Hu, *Oxidation degradation of polyphenylene sulfide needle felt at different sulfuric acid dew point temperatures*. High Performance Polymers, 2015. **27** (1): p. 94-99.
30. Tanthapanichakoon, W., et al., *Degradation of semi-crystalline PPS bag-filter materials by NO and O<sub>2</sub> at high temperature*. Polymer Degradation and Stability, 2006. **91** (8): p. 1637-1644.
31. Fukui, K., et al., *Effects of NO<sub>2</sub> gas concentration on the degradation of polyphenylene sulfide non-woven bag filter at high temperature*. Advanced Powder Technology, 2021. **32** (9): p. 3278-3287.
32. Lv, Y.-R., et al., *Polyphenylene sulfide (PPS) fibrous felt coated with conductive polyaniline via in situ polymerization for smart high temperature bag-filter*. Materials Research Express, 2019.**6** (7): p. 075706.
33. Xing, J., Z.Z. Xu, and B.Y. Deng, *Enhanced Oxidation Resistance of Polyphenylene Sulfide Composites Based on Montmorillonite Modified by Benzimidazolium Salt*. Polymers, 2018. **10** (1): p. 83.
34. Tan, S., et al., *A quantum chemical calculation study on crosslinking reaction mechanism of polyphenylene sulfide*. Journal of Chongqing University (Natural Science Edition), 1999(01): p. 108-113.
35. Youqin Hua, R.J., *Polymer physics* . 4th ed. 2013, Beijing: Chemical Industrial Press. 347.
36. Díez-Pascual, A.M. and M. Naffakh, *Synthesis and characterization of nitrated and aminated poly(phenylene sulfide) derivatives for advanced applications*. Materials Chemistry and Physics, 2012. **131** (3): p. 605-614.
37. Jia, M. and C. Ling, *Factors of Affecting the Flue Gas Acid Dew Point Temperature and its Way of Calculation*. Industrial Boiler, 2003(06): p. 31-35.
38. P, M., *A Contribution to the Problem of the Action of Sulfuric Acid on the Dew Point Temperature of Flue Gases*. Chemical Engineering Technology, 1959. **31** : p. 345-350.